Published in final edited form as:
Science. 2011 June 10; 332(6035): 1322–1326. doi:10.1126/science.1199484.

Quantitative Phosphoproteomic Analysis Identifies the Adaptor Protein Grb10 as an mTORC1 Substrate that Negatively Regulates Insulin Signaling

Yonghao Yu[1], **Sang-Oh Yoon**[1,4], **George Poulogiannis**[2], **Qian Yang**[1,3], **Xiaoju Max Ma**[1,5], **Judit Villén**[1,6], **Neil Kubica**[1,7], **Gregory R. Hoffman**[1], **Lewis C. Cantley**[2], **Steven P. Gygi**[1,*], and **John Blenis**[1,*]

[1]Department of Cell Biology, Harvard Medical School, Boston, MA, 02115

[2]Division of Signal Transduction, Beth Israel Deaconess Medical Center, Boston, MA, 02215

[3]Harvard School of Dental Medicine, Boston, MA, 02115

Abstract

The evolutionarily conserved Ser-Thr kinase mTOR plays a critical role in regulating many pathophysiological processes. Functional characterization of the mTOR signaling pathways, however, has been hampered by the paucity of known substrates. We used large-scale quantitative phospho-proteomics experiments to define the signaling networks downstream of mTORC1 and mTORC2. Characterization of one mTORC1 substrate, the growth factor receptor-bound protein 10 (Grb10), showed that mTORC1-mediated phosphorylation stabilized Grb10, leading to feedback inhibition of the phosphatidylinositol-3-kinase (PI3K) and extracellular signal-regulated, mitogen-activated protein kinase (ERK-MAPK) pathways. Grb10 expression is frequently downregulated in various cancers, and loss of Grb10 and loss of the well-established tumor suppressor phosphatase PTEN appear to be mutually exclusive events, suggesting that Grb10 might be a tumor suppressor regulated by mTORC1.

The evolutionarily conserved Ser-Thr protein kinase mTOR functions as the core catalytic component of two structurally and functionally distinct signaling complexes. mTOR complex 1 (mTORC1) regulates protein translation, autophagy and cell growth whereas mTOR complex 2 (mTORC2) regulates the actin cytoskeleton and cell survival (1–3). mTORC1 and mTORC2 respond to upstream inputs such as growth factors, energetic status, and amino acid levels (3) but relatively few downstream targets of mTOR have been identified.

Misregulated mTOR activity is a common feature of most cancers (1) but clinical trials evaluating the mTORC1 selective inhibitor rapamycin as an anti-cancer agent have met with limited success (2). Rapamycin resistance has emerged as a major challenge to its clinical use (4), and is caused in part by feedback loops that activate the PI3K and ERK-MAPK signaling pathways in rapamycin treated cells through poorly understood mechanisms (5, 6). Identifying substrates of mTORC1 and mTORC2 will be important for understanding how mTOR signals downstream, and for defining components of feedback loops involved in rapamycin resistance.

*To whom correspondence should be addressed. Steven_gygi@hms.harvard.edu (S.P.G); john_blenis@hms.harvard.edu (J. B.).
[4]Current address, Department of Cancer and Cell Biology, University of Cincinnati, College of Medicine, Cincinnati, OH, 45267
[5]Current address, Department of Research Oncology Diagnostics, Genentech Inc., 1 DNA Way, South San Francisco, CA, 94080
[6]Current address, Department of Genome Sciences, University of Washington, Seattle, WA, 98195
[7]Current address, Developmental and Molecular Pathways, Novartis Institutes for Biomedical Research, Cambridge, MA, 02139

We performed two sets of large-scale, quantitative phospho-proteomics experiments to characterize the signaling network downstream of mTOR (Figs. 1, S1, S2 and S3). The first stable isotope labeling with amino acids in cell culture (SILAC) experiment (Rapa screen) was performed using *Tsc2* −/− mouse embryonic fibroblasts (MEFs) (see supplemental text for detailed description of the screen). We identified 4,484 and 6,832 unique phosphorylation sites on 1,615 and 1,866 proteins from two biological replicate experiments, respectively (Table S1, Databases S1 and S2).

Several hundred peptides corresponding to 85 and 147 proteins in the two replicates (Database S3 and Fig. S1) were determined to contain rapamycin-sensitive phosphorylation sites (defined as phosphorylated peptides in control cells whose abundance were more than twice that in samples from rapamyin-treated cells). Many known effectors of the canonical mTORC1 signaling pathway were identified in the downregulated population, including p70S6K, 4EBP1/2, Akt1s1 (PRAS40), rpS6, eIF4B, eIF4G1 and GSK3β (Table S2, Figs. 1C and 1D). A representitive identification of the known rapamycin-sensitive phosphorylation sites on rpS6 is shown in Fig. 1B. In addition, the identification of many kinases, e.g. unc-51-like kinase 1 (ULK1), in the downregulated proteins provides potential points for signal integration and crosstalk (Table S2, see supplementary text and Table S3 for Gene Ontology (GO) analysis and detailed discussion of the hits).

Rapamycin is an allosteric inhibitor that only partially inhibits mTORC1 signaling and has no effect on the activity of mTORC2 under short-term treatment conditions (2). In contrast, ATP-competitive mTOR inhibitors block the activity of both mTORC1 and mTORC2 (1). To identify rapamycin-insensitive mTORC1, and mTORC2 substrates, we used the mTOR inhibitor Ku-0063794 and performed a second SILAC experiment (Ku screen) (Figs. 1A, 1C and S1). In this experiment, one hundred proteins were determined to contain downregulated phosphopeptides after Ku-0063794 treatment (Database S3, Table S2, see supplementary text for detailed discussion).

One of the enriched GO classes of hits in the Rapa screen is the receptor protein tyrosine kinase (RTK) signaling pathway ($P = 0.01$, Table S3), suggesting that mTORC1 might modulate its upstream regulators by altering the activities of RTKs. In particular, phosphorylation of S501 and S503 on the growth factor receptor-bound protein 10 (Grb10) was strongly inhibited by a 2-hr rapamycin treatment (Figs. 2A and S4A, Table S2). The intensity of a triply phosphorylated Grb10 peptide (T76, S96 and S104) also decreased after rapamycin treatment (Table S2).

We developed a phospho-specific antibody (Figs. S5A and S5B) and found rapamycin treatment induced rapid dephosphorylation of Grb10 at S501 and S503 (Fig. 2B). Grb10 phosphorylation was also decreased in *Tsc2* −/− MEFs deprived of amino acids (Fig. 2C). To determine whether S501 and S503 of Grb10 can be phosphorylated by other kinases, we treated *Tsc2*−/− cells with staurosporine, a broad-spectrum kinase inhibitor that, however, does not suppress mTOR activity (7). No change in the phosphorylation of Grb10 was observed (Fig. 2D). S6K activity was inhibited by staurosporine treatment, as shown by a complete loss of rpS6 phosphorylation, suggesting that Grb10 was directly phosphorylated by mTORC1 rather than by S6K.

In wt MEFs, insulin or serum stimulation increased Grb10 phosphorylation in a rapamycin-sensitive manner (Fig. 2E). Akt inhibition also reduced Grb10 and S6 phosphorylation. Grb10 S503 can be phosphorylated by ERK *in vitro* (8). Inhibition of the ERK-activating kinase, MEK with AZD6244 abolished phosphorylation of ERK but had no effect on phosphorylation of Grb10 (Fig. 2E), indicating that phosphorylation of S501 and S503 on Grb10 is not mediated by ERK *in vivo*. All other mTOR catalytic inhibitors tested, including

LY294002, NVP-BEZ235, torin and pp242 (9), also completely abolished Grb10 phosphorylation (Fig. 2F).

To examine a potential interaction between Grb10 and the mTOR complexes *in vivo*, we expressed HA-tagged Grb10 with Myc-tagged raptor or rictor in human embryonic kidney (HEK) 293T cells. Grb10 interacted with raptor, but not rictor, indicating that Grb10 is a binding partner of mTORC1, but not mTORC2 (Fig. 3A). Grb10 was also phosphorylated by recombinant mTOR at S501 and S503 *in vitro* (Fig. 3B).

Grb10 was much more abundant in *Tsc2*−/− and *Tsc1*−/− MEFs than in their wild-type counterparts (Figs. 3C and S5C) and the initial loss of Grb10 phosphorylation as a result of rapamycin treatment was followed by a decrease in Grb10 abundance and a smaller decrease in amount of Grb10 mRNA (Fig. 3D). Exposure to a proteosome inhibitor MG-132 suppressed rapamycin-induced Grb10 protein degradation (Fig. S5D). These results show that mTORC1 functions to promote accumulation of Grb10 both transcriptionally and post-translationally. Depletion of the mTORC1 component raptor also led to decreased abundance of Grb10 protein (Fig. 3E). Furthermore, long-term treatment with mTOR catalytic inhibitors led to reduced levels of Grb10 in *Tsc2*−/− MEFs (Fig. S5E), *Tsc1*−/− MEFs (Fig. S5F) and HeLa cells (Fig. S5G).

To explore whether Grb10 S501 and S503 phosphorylation contributed to its stabilization and high expression, we transfected wt-Grb10, Grb10-S501A–S503A (AA) and Grb10-S501D–S503D (DD) into HEK293T cells. Exogenous wt and DD Grb10 proteins were expressed in similar amount, but the AA mutant of Grb10 was less abundant, perhaps due to protein instability (Fig. 3F). To confirm this result, we generated *Tsc2*−/− MEFs stably expressing the HA-tagged Grb10-DD. Long-term rapamycin treatment of these cells decreased amounts of the endogenous, wt Grb10 but had no effect on the abundance of the DD mutant protein (Fig. 3G). This result appears not to result from protein overexpression, because in *Tsc2*−/− cells expressing HA-tagged wt Grb10, rapamycin treatment decreased the abundance of both the endogenous and ectopically expressed Grb10 (Fig. S5H). These data support a critical role for mTORC1 in stabilizing Grb10 through phosphorylation of the S501 and S503 residues. It is important to note that phospho-Akt levels still increased in these cells (Fig 3G), likely resulting from increased IRS1 levels after prolonged rapamycin treatment.

Grb10 functions as a negative regulator of insulin signaling. In Grb10 null mice, PI3K-Akt pathway hyperactivation was observed in insulin-sensitive tissues (10, 11). We therefore examined the possibility that mTORC1-mediated Grb10 phosphorylation and accumulation activated a negative feedback loop from mTORC1 to the PI3K-Akt pathway. The PI3K-Akt and ERK-MAPK pathways were both refractory to insulin or IGF stimulation in *Tsc2*−/− cells, as a result of constitutively elevated mTORC1 signaling (5, 6). In contrast, phosphorylation of both Akt and ERK was increased in Grb10-depleted cells deprived of serum or stimulated with insulin or IGF (Figs. 4A and S6A). Conversely, overexpression of Grb10 in HEK293 cells suppressed activation of PI3K (Fig. S6B) by inhibiting insulin receptor-dependent phosphorylation of insulin receptor substrate (IRS) and its subsequent recruitment of PI3K (Figs. S6C and S6D) (12). Knockdown of Grb10 in *Tsc2*−/− MEFs to a level close to that in wt cells did not completely restore the sensitivity of PI3K to insulin stimulation (Fig. S6E), suggesting additional mechanisms (e.g. lower IRS levels in *Tsc2*−/− MEFs) contribute to the feedback inhibition (Fig. S6F). Our data complement the previous findings and suggest that activation of mTORC1-S6K promotes negative feedback inhibition of PI3K through a two-prong mechanism: first, mTORC1-S6K-mediated phosphorylation and degradation of a positive regulator of PI3K signaling, IRS (6, 13, 14); second,

mTORC1-mediated phosphorylation and accumulation of a negative regulator of PI3K signaling, Grb10.

We next asked if PI3K activation in Grb10-depleted cells would promote survival against stress-induced apoptosis. In response to either staurosporine or etoposide, reduced caspase 3 cleavage was observed in Grb10 knockdown cells compared to that of control cells, indicating that Grb10 depletion is sufficient to protect cells from apoptosis (Figs. 4B and S6G). Because rapamycin can protect cells from energy stress-induced death (15), these results provide additional possible explanations for the cytostatic rather than cytotoxic effects of rapamycin in some cancers, and suggest a complete understanding of the feedback inhibition control will be critical in designing combination therapies involving rapamycin analogues.

Comprehensive meta-analysis of published microarray data revealed that the abundance of *GRB10* was decreased in many tumor types compared to that in normal tissue counterparts (Fig. 4C). Given that loss of Grb10 results in activation of the PI3K-Akt pathway (Fig. 4A), we performed correlation analysis and found that there was a significant ($p < 0.05$) negative correlation between *GRB10* and *PTEN* expression (Figs. 4D and 4E). This correlation was only observed in tumor samples but not in normal tissue controls (Fig. 4E). *PIK3CA* mutations and *PTEN* loss are mutually exclusive in breast cancer (16), suggesting that increased abundance of PIP_3 resulting from of genetic alteration of either *PIK3CA* or *PTEN* relieves selective pressure targeting the other gene. Similarly, loss of Grb10, which results in PI3K activation, might provide the cells with growth and survival advantages that are redundant with respect to PTEN loss-of-function, suggesting that Grb10 might be a tumor suppressor that is regulated by mTORC1. These data point to the prospect of targeting Grb10 stability in cancer therapy.

Materials and Methods

Cells and Reagents

Human embryonic kidney (HEK) 293 cells, HeLa and immortalized *Tsc1*+/+, *Tsc1*−/−, *Tsc2*+/+ and *Tsc2*−/− mouse embryonic fibroblasts (MEFs) (a kind gift from David Kwiatkowski, Brigham and Women's Hospital) were maintained in Dulbecco's modified Eagle's medium (DMEM) supplemented with 10% fetal bovine serum. In collaboration with Millipore Inc., we generated anti-phospho-S501/S503-Grb10 antibodies (Catalogue number 07-1520). Anti-mTOR, anti-phospho-mTOR (S2481), anti-phospho-Akt (S473), anti-phospho-Akt (T308), anti-Akt, anti-S6K, anti-phospho-S6K (T389), anti-IRS1, anti-IRS2, anti-PARP, anti-caspase 3, anti-4EBP, anti-4EBP (T37/T46), anti-phospho-ribosomal protein S6 (S235/S236), and anti-ribosomal protein S6 antibodies were obtained from Cell Signaling Technology. Anti-phospho-ERK1/2 antibody, insulin, Phorbol Myristate Acetate (PMA), Epidermal Growth Factor (EGF) and polybrene were purchased from Sigma. Anti-Grb10 (mouse), anti-phospho-IRS (Y612), anti-p85 and anti-p110 of PI3K antibodies were purchased from Santa Cruz, Invitrogen, Millipore and BD, respectively. ERK1/2 antibody and anti-HA antibody were prepared in the lab. LY294002 and AktVIII inhibitor were purchased from Calbiochem. Lipofectamine 2000 was purchased from Invitrogen. Torin was kindly provided by Nathanael Gray (Dana Farber Cancer Institute).

SILAC cell culture

Tsc2−/− MEFs were used in the Rapa screen due to constitutive hyperactivation of mTORC1 signaling in this cell line. Cells were grown in light ($[^{12}C_6{}^{14}N_2]$Lys, $[^{12}C_6{}^{14}N_4]$Arg) and heavy ($[^{13}C_6{}^{15}N_2]$Lys, $[^{13}C_6{}^{15}N_4]$Arg) DMEM (Cambridge Isotope Labs), respectively. Both light and heavy DMEM were supplemented with 10% dialyzed

FBS (Invitrogen). Cells were serum-deprived for 17 hours and cells were cultured in heavy media were treated with 20 nM rapamycin for two hours. We performed two biological replicates of this experimental design with cross-labeling (swapping the labeled state of the rapamycin-treated cells). For the purposes of illustration, the data for biological replicate #2 is presented in Figures.

The Ku screen was performed using wild-type (WT) MEFs. Cells were grown in the SILAC media described above. Both the light and heavy cells were starved of serum for 17 hrs. The light cells were treated with 20 nM rapamycin for 2 hrs, while the heavy cells were treated with a combination of 20 nM rapamycin and 2 μM Ku-0063794 for 2 hrs. Both the light and heavy cells were then stimulated with 100 nM insulin for 15 min.

Sample preparation for mass spectrometric analysis

The heavy and light cells were lysed in urea buffer (8 M urea, 20 mM HEPES pH 7.0, 75 mM β-glycerolphosphate, 1 mM sodium vanadate, 1 mM DTT and 1.5 mM EGTA) and the lysates were combined at a 1:1 ratio. Lysates were reduced by adding DTT to a final concentration of 3 mM, followed by incubation at room temperature for 20 min. Cysteines were alkylated by adding iodoacetamide to a final concentration of 50 mM, followed by incubation in the dark for 20 min. The lysates were diluted to a final concentration of 2 M urea by addition of 100 mM NH_4OAC (pH 6.8) and were digested overnight with sequencing-grade trypsin (Promega) at a 1:100 (enzyme:substrate) ratio. Digestion was quenched by addition of trifluoroacetic acid to a final concentration of 0.1% and precipitates were removed by centrifugation at 4,000 rpm for 30 min. Peptides were desalted on SepPak C18 columns (Waters) according to manufacturer's instructions.

Phosphopeptides were enriched by SCX-IMAC (1). Briefly, lyophilized peptides were resuspended in 500 μl SCX buffer A (5 mM KH_2PO_4, pH 2.65, 30% acetonitrile) and injected onto a SCX column (Polysulfoethyl aspartamide, 9.4 mm×200mm, 5 μM particle size, 200 Å; pore size, PolyLC). Gradient was developed over 35 min ranging from 0% to 21% buffer B (5 mM KH_2PO_4, pH 2.65, 30% acetonitrile, 350 mM KCl) at a flow rate of 2 ml/min. Twelve fractions were collected and lyophilized. Peptides were then desalted using SepPak C18 columns and were subjected to IMAC (Sigma) for phosphopeptide enrichment. The eluate was further desalted using STAGE tips (2) and lyophilized.

Mass spectrometry analysis and data processing

The Rapa screen samples were analyzed by LC-MS/MS on an LTQ-Orbitrap mass spectrometer (Thermo, San Jose, CA) using the top ten method (3). The Ku screen samples were analyzed on an LTQ-Velos mass spectrometer (Thermo Fischer Scientific, San Jose, CA) using the top twenty method. MS/MS spectra were searched against a composite database of the mouse IPI protein database (Version 3.60) and its reversed complement using the Sequest algorithm. Search parameters allowed for a static modification of 57.02146 Da for Cys and a dynamic modification of phosphorylation (79.96633 Da) on Ser, Thr and Tyr, oxidation (15.99491 Da) on Met, stable isotope (10.00827 Da) and (8.01420 Da) on Arg and Lys, respectively. Search results were filtered to include <1% matches to the reverse data base by the linear discriminator function (Huttlin et al., manuscript in preparation) using parameters including Xcorr, dCN, missed cleavage, charge state (exclude 1+ peptides), mass accuracy, all heavy or light Lys and Arg, peptide length and fraction of ions matched to MS/MS spectra. Phosphorylation site localization was assessed by the Ascore algorithm (4) based on the observation of phosphorylation-specific fragment ions and peptide quantification was performed by using the Vista algorithm (3, 5).

We further filter the peptides according to the following criteria for quantitation of the peptide abundance changes: (1) Vista confidence score must be at least 85, (2) signal to noise ratio (S/N) ≥ 3 for both the heavy and light peptides, (3) in the cases where one of the isotopic species has an S/N of ≤ 3, S/N of the other was required to be ≥ 5, and (4) in the cases where only the heavy or light version of a peptide was found, we reported the peak S/N ratio, or its inverse, as a proxy for relative abundance measurement. For such peptides, we also required S/N of at ≥ 5 for the observed species. The complete original datasets and the ones filtered based on the aforementioned criteria for the Rapa and Ku screens are provided in supplementary databases S1 and S3, respectively.

Plasmids

The cDNA for human Grb10 (NCBI gene symbol GRB10; Gene ID: 2887) was obtained from Invitrogen and amplified by PCR. The product was subcloned into (1) the BamH I and EcoR I sites of pKH3, (2) the BamH I and EcoR I sites of pGEX-4T-3 or (3) the Hind III and EcoR I sites of pLPCX. The Grb10 point mutant constructs were generated using the QuickChange site-directed mutagenesis kit (Stratagene). pRK5-Myc-raptor and pRK5-Myc-rictor were kindly provided by David Sabatini (MIT). Lentiviral plasmids (Δ8.9 and VSVG) were kind gifts from Andrew Kung (Dana Farber Cancer Institute) and David Baltimore (California Institute of Technology).

Immunoprecipitation

Cells were extracted with lysis buffer A (40 mM HEPES, pH 7.5, 120 mM NaCl, 1 mM EDTA, 10 mM β-glycerophosphate, 50 mM NaF, 2 mM phenylmethylsulfonyl fluoride, 2 mg/ml aprotinin, 2 mg/ml leupeptin, and 1mg/ml pepstatin, 1mM DTT) containing 1% Triton X-100 and 1% NP-40. After centrifugation, supernatants were collected and pre-cleared for 1 h with protein A- and G-Sepharose beads (GE Healthcare Biosciences). After centrifugation at 3,000 rpm for 5 min, the supernatants were incubated with the antibody at 4°C for 2 h, and then incubated with protein A- and G-Sepharose for an additional hour. Beads were washed four times with the lysis buffer and eluted in 2× reducing sample buffer.

Mammalian lentiviral shRNAs

Lentiviral short hairpin RNA (shRNA) expression vectors were a kind gift from William Hahn (Dana Farber Cancer Institute). To generate the lentiviruses, shRNA plasmids were co-transfected into HEK293TD cells along with packaging (Δ8.9) and envelope (VSVG) expression plasmids using lipofectamine 2000 (Invitrogen). Two days after transfection, viral supernatants were harvested and filtered. Recipient cells were infected in the presence of a serum-containing medium supplemented with 8 μg/ml polybrene. Following infection for 36 h, cells were treated with 2.0 μg/ml puromycin (Sigma) and cell lines that stably expressed the shRNAs were selected. Knockdown efficiencies were examined by immunoblot assay using antibodies against the target protein.

Immunoblot analysis

For immunoblot analysis, the cells were extracted in lysis buffer (20 mM HEPES pH 7.5, 1% Triton X-100, 150 mM NaCl, 10 mM EDTA, 1 mM EGTA, 1 mM sodium orthovanadate, 1 mM NaF, 2 mM phenylmethylsulfonyl fluoride, 2 mg/ml aprotinin, 2 mg/ml leupeptin, and 1mg/ml pepstatin), and extracts were mixed with the 5X reducing buffer (60 mM Tris-HCl, pH 6.8, 25% glycerol, 2% SDS, 14.4 mM 2-mercaptoethanol, 0.1% bromophenol blue). Samples were boiled for 5 min and subject to electrophoresis using the standard SDS-PAGE method. Proteins were then transferred to a nitrocellulose membrane (Whatman). The membranes were blocked with a TBST buffer (25 mM Tris-HCl, pH 7.5, 150 mM NaCl, 0.05% Tween 20) containing 3% nonfat dried milk, and probed overnight

with primary antibodies at 4 °C and for 1h at RT with peroxidase-conjugated secondary antibodies. Blots were developed using enhanced chemiluminescence, exposed on autoradiograph film and developed using standard methods. Western blot images were quantified by using the software package ImageJ.

Recombinant protein purification

For the purification of GST-tagged proteins, plasmids were transformed into *Escherichia coli* strain BL21 (DE3), and purified to homogeneity from crude lysates using glutathione-sepharose beads (GE Healthcare) according to the manufacture's protocol. Briefly, protein production was induced by adding isopropyl-D-thiogalactopyranoside (Sigma) to the cultures. Bacteria were collected by centrifugation, resuspended in PBS and lysed by sonication. After centrifugation at 13,000 rpm for 15 min, the supernatant was incubated with glutathione-sepharose beads for 1 h. The beads were washed with PBS three times and the recombinant protein was eluted with PBS containing 20 mM reduced glutathione. Proteins were dialyzed against PBS and stored at −80 °C until use.

mTOR kinase assay

Grb10 was phosphorylated by mTOR *in vitro*. Recombinant GST-Grb10 was purified in *E. Coli* and recombinant mTOR was purchased from Calbiochem. GST-Grb10 was incubated with or without mTOR in 50 μl reaction mixture at 37°C for 30 mins. The reaction mixture contained 1X mTOR kinase buffer (Invitrogen), 1X protease inhibitor cocktail (Roche), 2 mM DTT, 10 μM ATP, 1 μg GST-Grb10, and 250 ng mTOR when indicated. Reaction was stopped by adding 16 μl of 4X SDS sample buffer and boiling at 100°C for 5 mins.

S6K1 was phosphorylated by mTOR *in vitro*. HA-S6K1 was purified from HEK 293 cells by immunoprecipitation. Specifically, 1 μg of HA-S6K1 was transfected into 5×10^6 HEK 293 cells on a 10 cm plate. Before harvesting, cells were treated with 20 ng/ml rapamycin for 1 hr. Cells were lysed in 0.3% CHAPS buffer and HA-S6K1 was immunoprecipitated by 30 μl pre-washed HA-conjugated resin (Covance). The resin with HA-S6K1 was equilibrated with the 1X mTOR kinase buffer before the reaction. The *in vitro* kinase reactions were assembled and carried out as described above except HA-S6K1 was used as the substrate instead of GST-Grb10.

RSK was phosphorylated by ERK2 but not mTOR. Recombinant GST-RSK was purified from *E. Coli*. Recombinant activated GST- ERK2 was purchased from Upstate. Two micrograms of GST-RSK was incubated with either ERK2 (1 μg) or mTOR, or without a kinase using the same reaction conditions and procedures as described above.

Reactions mixtures were resolved on 10% SDS-PAGE and transferred to nitrocellulose membrane. Western blots were carried out following a standard protocol, using 5% non-fat milk in TBST, antibodies (anti-GST, Santa Cruz; anti-HA, anti-mTOR, anti-pT389 S6K1, Cell Signaling; anti-pT573 RSK, R&D) as indicated, HRP-conjugated secondary antibodies and ECL. GST-ERK2 and GST-RSK were visualized by coomassie blue staining.

Quantitative RT-PCR analysis

Total cellular RNA was purified from cultured cells using the RNeasy mini kit (Qiagen) following the manufacturer's protocol. For quantitative real-time PCR (qRT-PCR), RNA was reverse-transcribed using the High-Capacity cDNA Reverse Transcription Kit (Applied Biosystems) according to the manufacturer's instructions. The resulting cDNA was analyzed by qRT-PCR using the QuantiTect SYBR Green qPCR System (Qiagen). A QuantiTect Primer Assay for mouse Grb10 was used to amplify the target gene, while the β-actin primers (β-actin forward, ACCCAGATCATGTTTGAGACCT; and β-actin reverse,

GCAGTAATCTCCTTCTGCATCC) were used as a normalization control. All reactions were run on an ABI 7900HT Fast Real-Time PCR instrument with a 15 min hot start at 95°C followed by 40 cycles of a 3-step thermocycling program: denaturation: 15 s at 94°C, annealing: 30 s at 55°C and extension: 30 s at 70°C. Melting curve analysis was performed at the end of every run to ensure that a single PCR product of the expected melting temperature was produced in a given well. A total of 3 biological replicates × 4 technical replicates were performed for each treatment group. Data was analyzed using the comparative C_t method ($\Delta\Delta C_t$ method).

Analysis of *GRB10* and *PTEN* expression in human samples

The Oncomine cancer microarray database was used for the expression analysis. We found that GRB10 mRNA expression was significantly downregulated in cancer vs. normal tissue in at least three independent microarray studies. Microarray expression data from six independent data sets corresponding to patient samples from bladder (GSE3167), glioblastoma (GSE4536), breast (GSE5764), myeloma (GSE5900) and pancreatic (GSE1542) carcinoma as well as data from matching normal tissues were downloaded from Gene Expression Omnibus (http://www.ncbi.nlm.nih.gov/geo/) and for prostate carcinoma from the Broad Institute cancer program datasets (http://www.broadinstitute.org/cgi-bin/cancer/datasets.cgi). The correlation in the gene expression between *GRB10* and *PTEN* was performed using Pearson's correlation coefficient analysis and the samples were clustered using the Euclidean distance metric and Ward's linkage algorithm.

Supplementary Material

Refer to Web version on PubMed Central for supplementary material.

Acknowledgments

We thank members of the Blenis and Gygi labs for critical discussion. This work was supported by a postdoctoral fellowship from the Tuberous Sclerosis Alliance, Grant ID-146 (Y.Y.), and grants from NIH GM051405 and CA46595 (J. B.), HG3456 (S. P. G.) and R00CA140789 (J. V.). J. B. is an Established Investigator of the LAM Foundation.

References

1. Alessi DR, Pearce LR, Garcia-Martinez JM. Sci Signal. 2009; 2:27.
2. Choo AY, Blenis J. Cell Cycle. 2009; 8:567. [PubMed: 19197153]
3. Ma XM, Blenis J. Nat Rev Mol Cell Biol. 2009; 10:307. [PubMed: 19339977]
4. Cloughesy TF, et al. PLoS Med. 2008; 5:e8. [PubMed: 18215105]
5. Carracedo A, et al. J Clin Invest. 2008; 118:3065. [PubMed: 18725988]
6. Shah OJ, Wang Z, Hunter T. Curr Biol. 2004; 14:1650. [PubMed: 15380067]
7. Choo AY, Yoon SO, Kim SG, Roux PP, Blenis J. Proc Natl Acad Sci U S A. 2008; 105:17414. [PubMed: 18955708]
8. Langlais P, et al. Biochemistry. 2005; 44:8890. [PubMed: 15952796]
9. Guertin DA, Sabatini DM. Sci Signal. 2009; 2:24.
10. Charalambous M, et al. Proc Natl Acad Sci U S A. 2003; 100:8292. [PubMed: 12829789]
11. Wang L, et al. Mol Cell Biol. 2007; 27:6497. [PubMed: 17620412]
12. Lim MA, Riedel H, Liu F. Front Biosci. 2004; 9:387. [PubMed: 14766376]
13. Tzatsos A, Kandror KV. Mol Cell Biol. 2006; 26:63. [PubMed: 16354680]
14. O'Reilly KE, et al. Cancer Res. 2006; 66:1500. [PubMed: 16452206]
15. Choo AY, et al. Mol Cell. 2010; 38:487. [PubMed: 20513425]

16. Saal LH, et al. Cancer Res. 2005; 65:2554. [PubMed: 15805248]

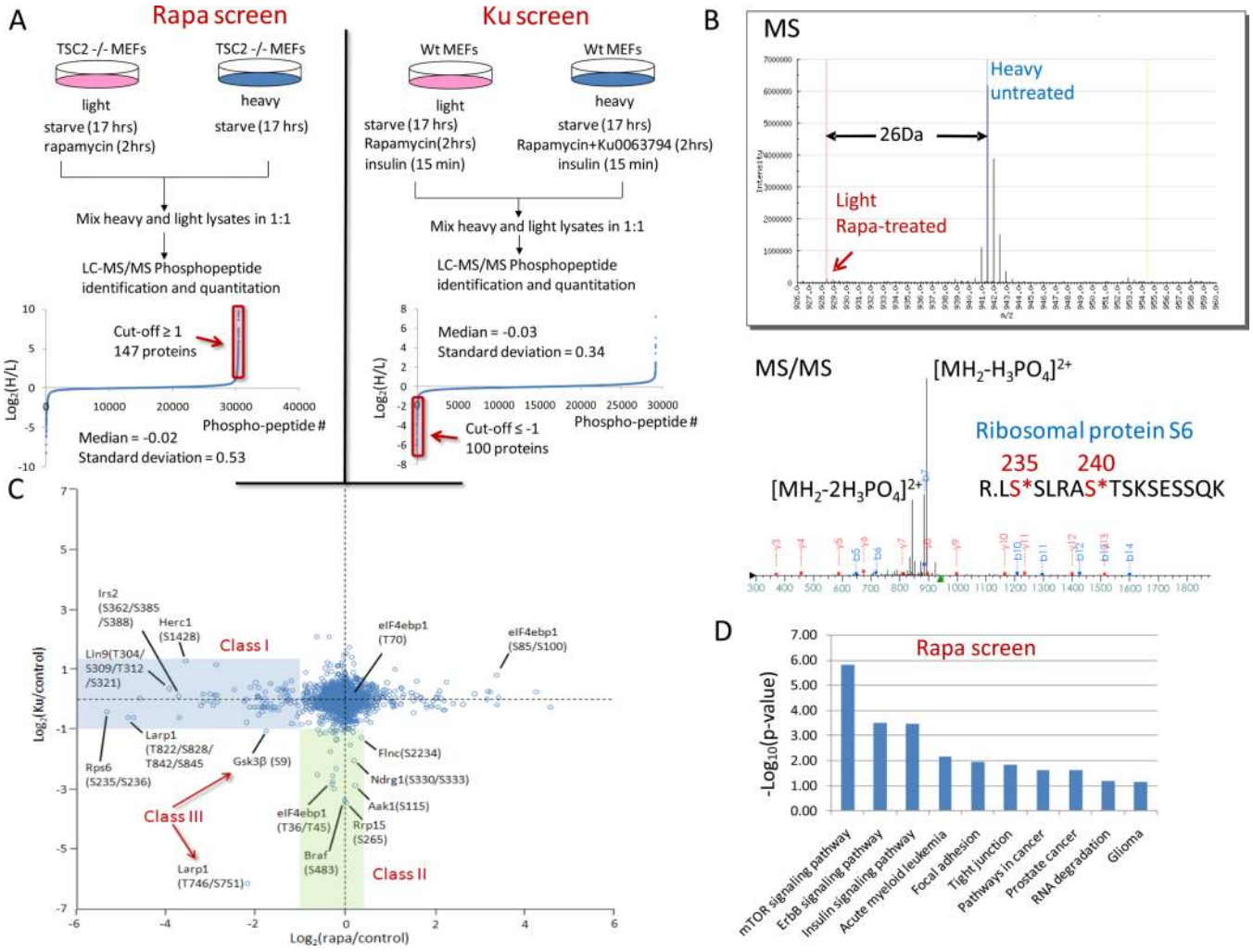

Fig. 1.

Sample preparation and data analysis for quantitative phosphoproteomic profiling of the mTOR downstream signaling networks. (A) Schematics of the two SILAC mass spectrometry experiments are shown with a plot highlighting the ratio distribution of phosphopeptides identified in each screen. (See data summary in Table S1). Note that most of the phosphopeptides have a ratio of 1:1 between the light and heavy populations and hence have a value close to 0 on a Log_2 axis. Proteins with downregulated phosphorylation in each screen are highlighted in the red box. (B) Typical MS and MS/MS spectra in which LS*SLRAS*TSKSESSQK from ribosomal protein S6 (S235 and S240) was identified as a rapamycin-sensitive phosphopeptide. The light and heavy peptides differ by 26 Da, corresponding to 2 labeled Lys and 1 labeled Arg in this particular peptide. (C) Quantitative differences between the rapamycin sensitive- and insensitive- mTOR downstream phosphorylation events. Phosphopeptides identified in both screens were extracted and their corresponding treatment/control ratios (See Table S1 for treatment conditions) were plotted on a Log_2 scale. Log_2(treatment/control) ≤ −1 is considered to be downregulated (See supplementary text for detailed discussion). (D) The top ten pathways enriched in the downregulated phospho-proteins identified in the Rapa screen.

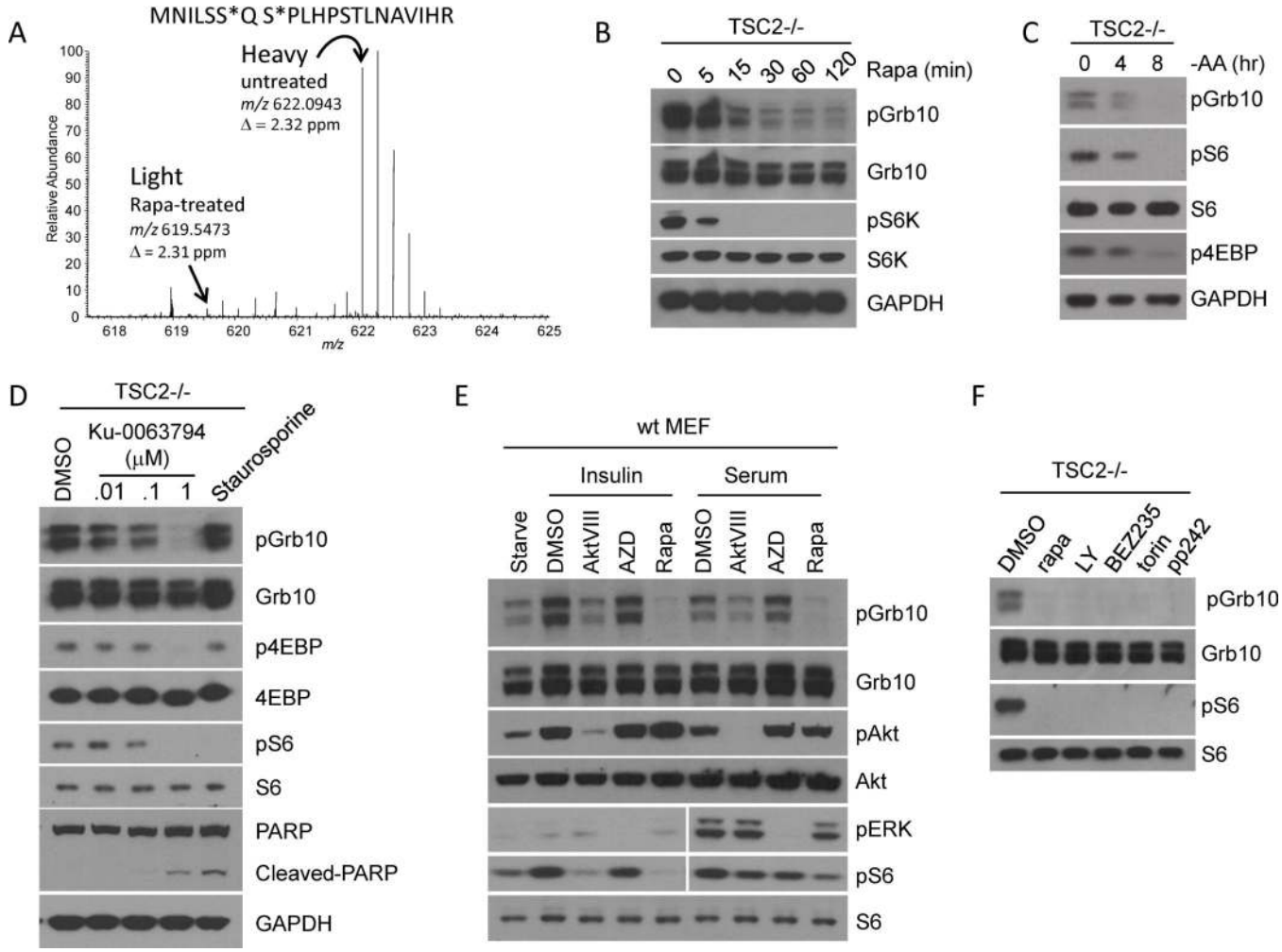

Fig. 2.

Sensitivity of phosphorylation of Grb10 at S501 and S503 to rapamycin inhibition (A) Identification of a doubly-phosphorylated, rapamycin-sensitive Grb10 peptide (MNILSS*QS*PLHPSTLNAVIHR, asterisk indicates the site of phosphorylation at S501 and S503). (B) Phosphorylation of Grb10 at S501 and S503 shows rapamycin sensitivity *in vivo*. *Tsc2*−/− cells were starved for serum and treated with 20 nM rapamycin for the indicated times. (C) Phosphorylation of Grb10 at S501 and S503 is sensitive to amino acids withdrawal. *Tsc2*−/− cells were serum-deprived in DMEM overnight and then transferred to a media of DMEM minus amino acids for the indicated times. (D) Phosphorylation of Grb10 at S501 and S503 is not affected by the pan-kinase inhibitor, staurosporine. *Tsc2*−/− cells were starved for serum and treated with either 100 nM staurosporine or Ku-0063794 at the indicated concentrations for two hours. (E) Grb10 phosphorylation is increased upon growth factor stimulation. wt MEFs were starved for serum overnight and then were stimulated with either insulin (100 nM) or serum (10%) for 15 min. Cells were preincubated with the indicated compounds for two hours. AktVIII (1 μM) and AZD (AZD6244, 5 μM) are specific inhibitors of Akt and MEK, respectively. Rapa (rapamycin) was used at 20 nM. (F) Grb10 phosphorylation at S501 and S503 is sensitive to various mTOR kinase inhibitors. *Tsc2*−/− cells were serum-starved and treated with the indicated compounds for two hours. The concentrations of the compounds were, Rapa (rapamycin) 20 nM, LY (LY294002) 20 μM, BEZ235 (NVP-BEZ235) 500 nM, torin 100 nM and pp242 1 μM. Phosphorylation

levels in this figure were measured with phospho-specific antibodies against Grb10 (S501, S503), S6K (T389), S6 (S235, S236), Akt (S473), 4EBP (T37, T46) and ERK1/2 (T202, Y204)

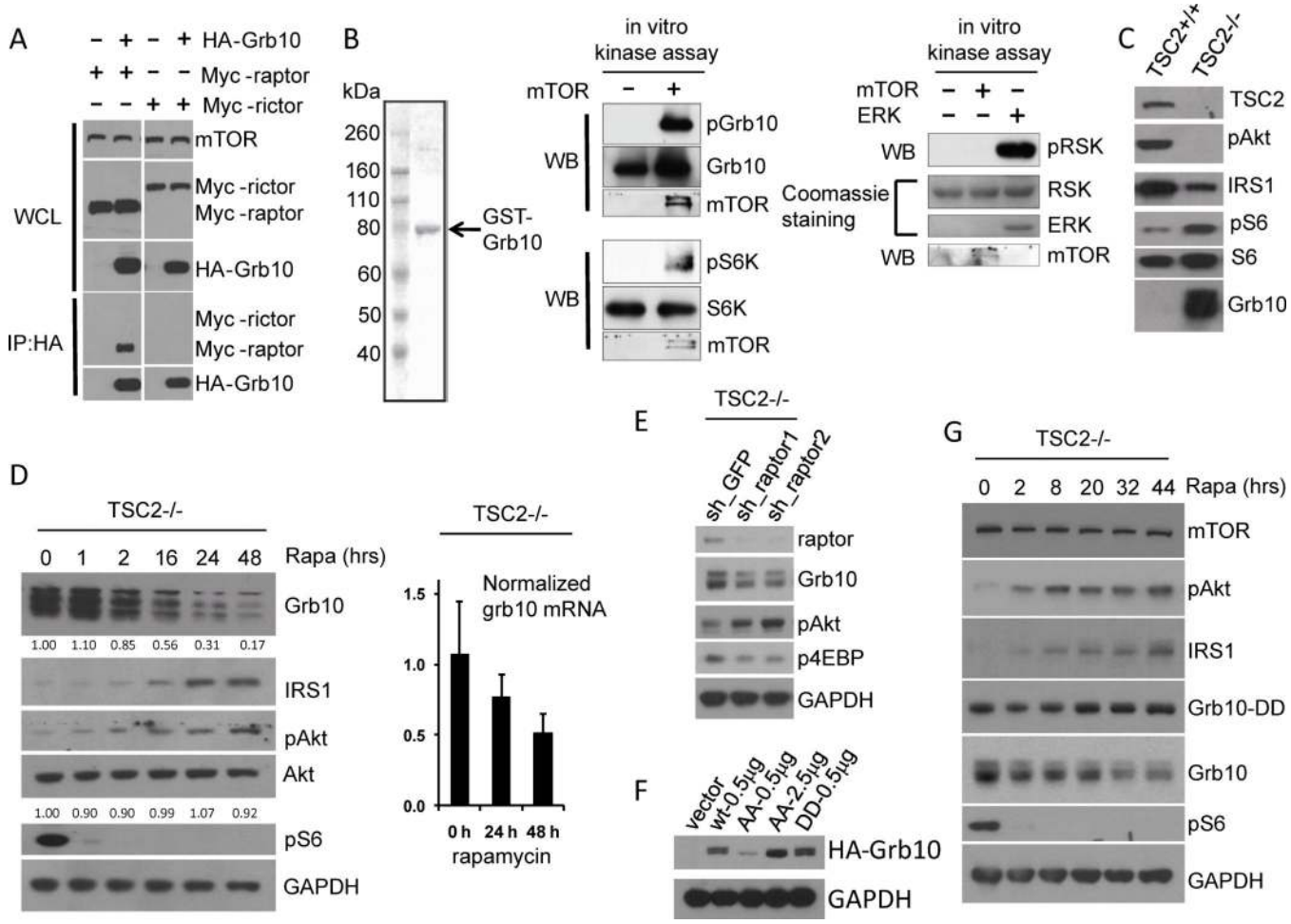

Fig. 3.

Effect of mTOR-mediated phosphorylation to promote stability of Grb10. (A) Grb10 interacts with raptor, but not rictor. HA-tagged Grb10 was transfected with Myc-raptor or Myc-rictor into HEK293T cells. Cells were lysed in lysis buffer A and the lysates were subjected to immunoprecipitation using anti-HA antibody conjugated beads. Raptor and rictor were probed with an antibody against the Myc-tag. WCL, whole cell lysates. (B) Grb10 is phosphorylated by mTOR *in vitro*. Recombinant GST-Grb10 was prepared from bacteria and was incubated with recombinant mTOR *in vitro*. Phosphorylation of Grb10 at S501 and S503 was detected by using the phospho-specific antibody against these two sites. S6K and RSK were used as the positive and negative controls, respectively and the experiments were performed in parallel with the mTOR-Grb10 *in vitro* kinase assay. WB, western blotting. (C) Grb10 is highly overexpressed in *Tsc2* −/− cells. (D) Long-term rapamycin treatment leads to Grb10 degradation in *Tsc2* −/− cells. Note that Grb10 protein expression levels inversely correlated with Akt activity. mRNA level was determined using quantitative RT-PCR based on three biological replicate experiments. (E) Knockdown of raptor in *Tsc2* −/− cells decreased Grb10 protein level. Cells were starved overnight and the lysates were probed with the antibodies indicated. (F) S501A–S503A mutant is unstable compared with the wild-type or the S501D–S503D mutant. The same amount of DNA was transfected into HEK293T cells. (G) Rapamycin failed to induce degradation of the S501D–S503D mutant. S501D–S503D mutant (DD) was stably expressed in *Tsc2* −/− cells and cells were treated with 20 nM rapamycin for the indicated times. Endogenous Grb10 was

detected using an antibody that preferentially recognizes mouse Grb10 whereas the Grb10 DD mutant (of human origin) was detected using an anti-HA antibody. Phosphorylation levels in this Figure were measured with phospho-specific antibodies against Grb10 (S501, S503), S6K (T389), RSK (T573), Akt (S473) and 4EBP (T37, T46).

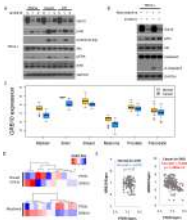

Fig. 4.

Grb10 is involved in the feedback inhibition loop from mTORC1 to PI3K and ERK-MAPK, and *GRB10* mRNA expression is decreased in abundance in many cancers and is negatively correlated with *PTEN* expression. (A) Knockdown of Grb10 in *Tsc2*−/− cells resulted in PI3K and ERK-MAPK hyperactivation after insulin or IGF stimulation. C, shGFP. 1, shGrb10 #1. 2, shGrb10 #2. Phosphorylation levels were measured against Akt (S473) and ERK1/2 (T202, Y204). (B) Knockdown of Grb10 in *Tsc2* −/− cells protected cells against apoptosis. Grb10 knockdown and control cells were starved overnight and then treated with 100 nM staurosporine for 5 hrs to induce apoptosis. Phosphorylation levels were measured against Akt (S473). (C) Box plots indicating that *GRB10* expression is significantly lower in many tumor types compared to their corresponding normal tissues. (Only the tumor types that showed significantly lower *GRB10* expression in cancer vs. normal in at least three independent microarray datasets are included, $p < 0.01$, Log-rank test). (D) Heat maps indicating a strong negative correlation between *GRB10* and *PTEN* expression in myelomas and breast carcinomas. Low levels of *GRB10* expression rarely occurred in tumors that also showed low levels of *PTEN* expression. The z-scores (from −1 to +1) of the normalized expression values for the corresponding cancer datasets on Fig 4C are shown. Red, lower expression compared to mean (white). Blue, higher expression compared to mean (white). (E) Scatter plots comparing the expression levels of *GRB10* and *PTEN* in the normal and tumor samples, collected from 6 different tissue types indicated in Fig. 4C. The negative correlation between *GRB10* and *PTEN* expression is evident in the tumor but not in the corresponding normal samples.